Cite as: F. De Luca, E. Chioccarelli, I. Iervolino (2011), *Preliminary study of the 2011 Japan earthquake ground motion record V1.01*, available at http://www.reluis.it.

PRELIMINARY STUDY OF THE 2011 JAPAN EARTHQUAKE (M 9.0) GROUND MOTION RECORDS V1.01

Flavia De Luca, Eugenio Chioccarelli and Iunio Iervolino

flavia.deluca@unina.it; eugenio.chioccarelli@unina.it, iunio.iervolino@unina.it

Dipartimento di Ingegneria Strutturale, Università di Napoli Federico II. Via Claudio 21, 80125, Naples, Italy.

1. Introduction

The Japan (Tohuku) earthquake that occurred on the 11th of March 2011 was the second one after the 2010 Chile earthquake (M 8.8) of the series of big earthquakes that followed the 2004 Sumatra earthquake (M 9.2) [Zollo A., 2011]. The USGS has updated the magnitude of the Tohoku earthquake in Northern Honshu, Japan, to 9.0 from the previous estimate of 8.9. Independently, Japanese seismologists have also updated their estimate of the earthquake's magnitude to 9.0. This magnitude places the earthquake as the fourth largest in the world since 1900 and the largest in Japan since modern instrumental recordings began 130 years ago [USGS, 2011].

Records from the main shock of the event have been released few hours later by different networks on the web, herein it is proposed a selection of station recordings that have been employed for the evaluation of peak and cyclic parameters and the elastic acceleration spectra. The selection of the stations was made on the basis of the maximum peak ground acceleration recorded.

2. Event

The event time is 05:46:23 UTC, and the epicentre coordinates are 38.322 N, 142.368 E, 129 km from Sendai, Honshu, Japan, [USGS, 2011]. The depth of the event was 24 km. Fault area is estimated in about 500x200 km^2. In Figure 1 is reported the shake map of the event according to USGS.

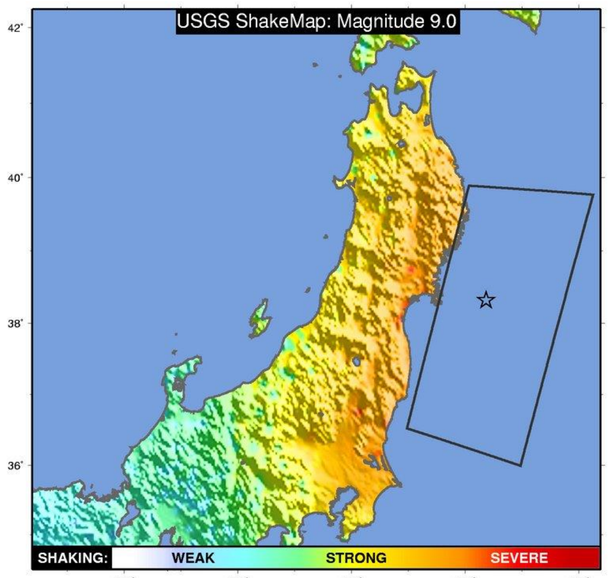

Figure 1. Bare shake map (map version 7 processed Wed Mar 16, 2011) available at *http://earthquake.usgs.gov/earthquakes/shakemap/global/shake/c0001xgp/*

3. Selected Recording Stations' Information

The stations considered are shown in Figure 2 and station details are shown in Table 1. The stations selected belong to three different networks: four stations are from K-Net network [http://www.k-net.bosai.go.jp/], four stations are from Kik-Net network [http://www.kik.bosai.go.jp/], two stations are from BRI strong motion observation network[1] [http://smo.kenken.go.jp/weblinks]. Records from K-Net are registered on surface, and the site soil profiles are available for all the station considered for at least 10 m (Table 2), all the three components have been considered (NS, EW, UD). Records from Kik-Net are registered on both surface and underground[2], for both conditions three components have been considered (NS, EW, UD) and difference in meters between surface and underground registration is also reported in Table 1. Records form BRI strong motion observation are placed on buildings at different levels, two station have been considered, *Sendai Government Office#2 at basement level* (BF2) and *Annex, Hachinohe City Hall at ground level* (GL), for each record the three components have been considered, the direction is the clockwise angle in degree from North (azimuth) for the horizontal components and up down for the third vertical component.

Records from K-Net and Kik-Net networks have been corrected employing a linear baseline correction and a Buttereworth bandpass filter (Freq1=0.1, Freq2=25, Order 4). BRI records have not been corrected since it was not necessary. Figure 2 shows epicentre location and the stations considered according to a colour legend to distinguish the networks.

[1] This network is explicitly devoted to dynamic monitoring of buildings.
[2] Height in meters is considered with respect to the sea level.

Table 1. Station location

Network	Station Code	Site Name	Lat	Lon	Surface	Underground	Difference
					m	***m***	***m***
Kik-Net	FKSH10	Nishigou	37.1585	140.0963	565	364	201
Kik-Net	FKSH19	Miyakoji	37.4672	140.7261	510	410	100
Kik-Net	MYGH10	Yamamoto	37.9381	140.8958	18	-187	205
Kik-Net	TCGH16	Haga	36.5449	140.0784	105	-7	112
K-Net	IBR003	Hitachi	36.5915	140.6453	57.5	/	/
K-Net	MYG004	Tsukidate	38.7292	141.0217	40	/	/
K-Net	MYG012	Shiogama	38.3175	141.0193	1.7	/	/
K-Net	MYG013	Sendai	38.2663	140.9293	5	/	/
BRI	SND	Sendai Government Office Bldg. #2	38.2669	140.8739	B2F	/	/
BRI	HCN2	Annex, Hachinohe City Hall	40.5117	141.4889	GL	/	/

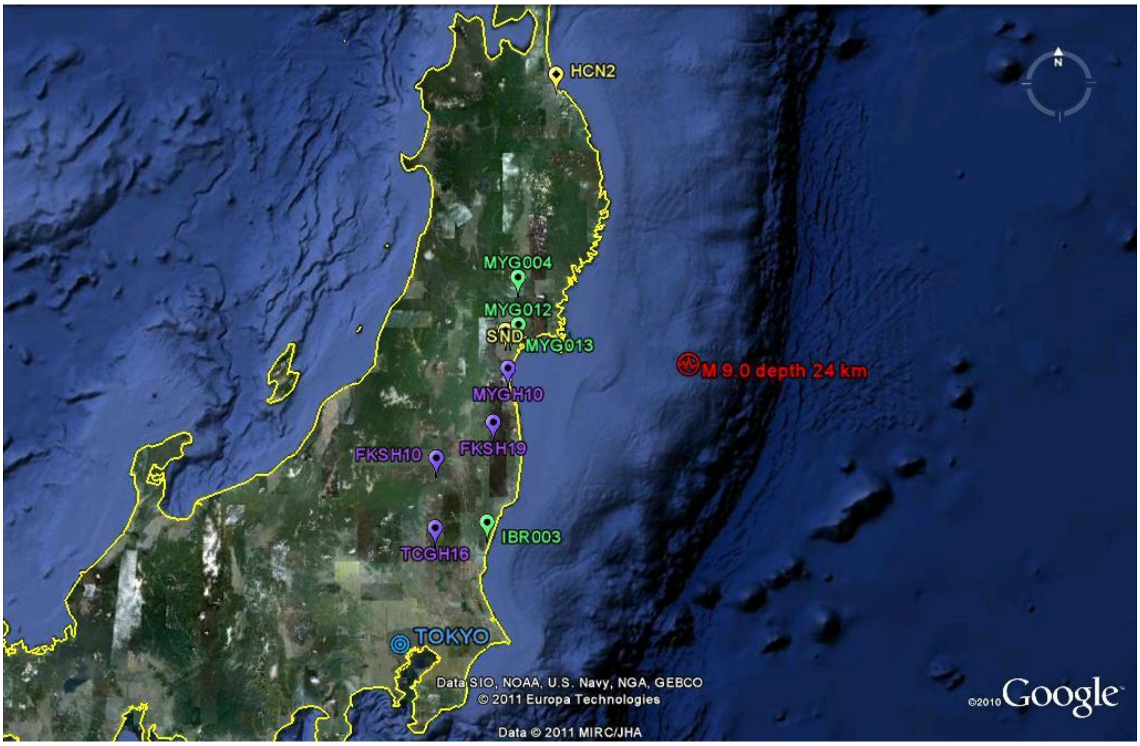

Figure 2. Selected stations from different networks, (green – K-net), (violet – Kik-net), (yellow, BRI strong motion observation),and epicentre localization, Google Earth.

Table 2. K-Net stations: velocity profiles and soil columns

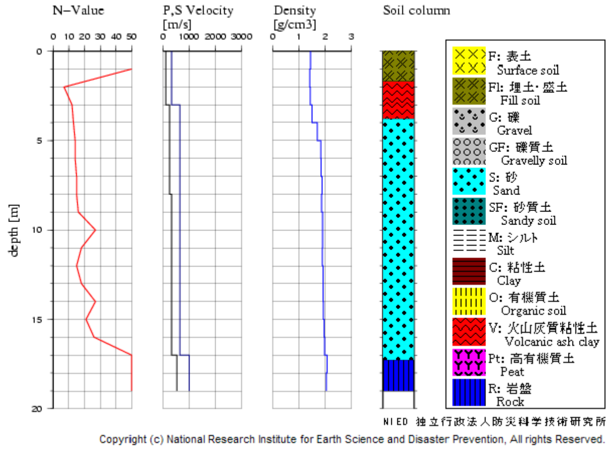

IBR003

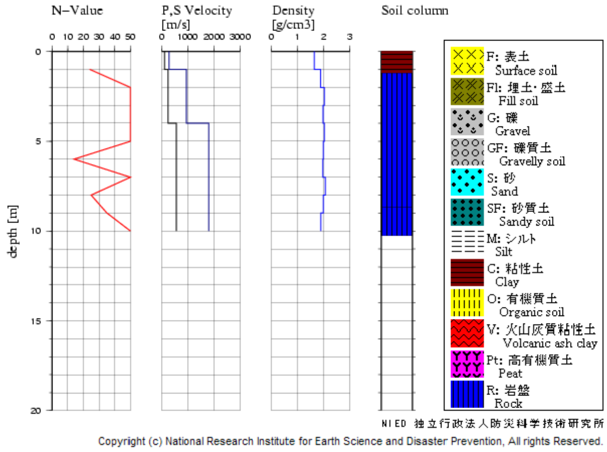

MYG004

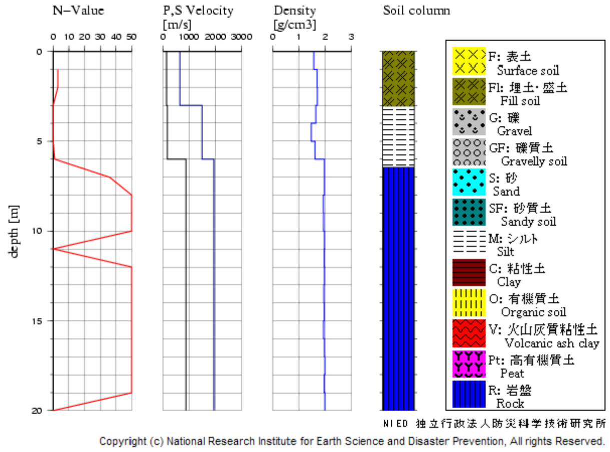

MYG012

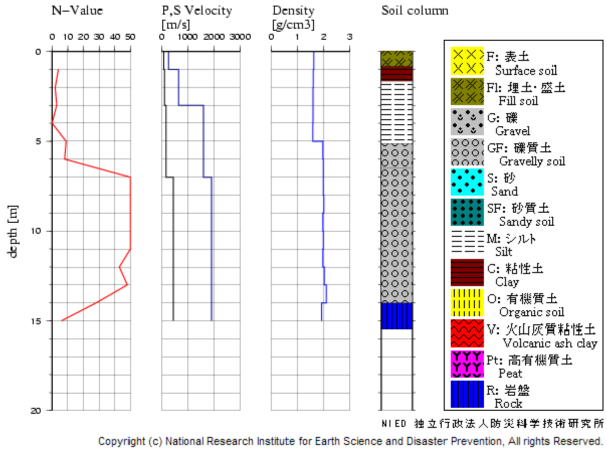

MYG013

4. Peak and Cyclic Parameters

Peak and cyclic parameters of ground motion have been evaluated for each record component. Peak parameters evaluated are the peak ground acceleration (PGA) and the peak ground velocity (PGV). The latter was evaluated only on the corrected records because of the necessity of baseline correction[3]. Cyclic parameters considered are the Arias intensity (IA), the Cosenza and Manfredi index (I_D) [Cosenza et al., 1993], defined in equation (1), and the significant duration (S_d), evaluated as the interval of time over which 5% to 95% of the total Arias intensity is accumulated.

$$I_D = \frac{2 \cdot g}{\pi} \frac{I_A}{PGA \cdot PGV} \tag{1}$$

For uncorrected records from Kik-Net and K-Net (see Table 3 and Table 4), three values of peak ground acceleration are reported: PGA, evaluated from our own processing of the record; PGAk, evaluated from our own processing according to the standard of K-Net and Kik-Net, considering the peak value minus the average of the acceleration of the record; and PGAr, that reported in the

[3] Since I_D is affected by PGV it was evaluated only for corrected waveforms.

record file. For corrected records from Kik-Net and K-Net and records from BRI network (see Table 5, Table 6 and Table 7), the PGAk is not evaluated and PGV and I_D value are shown.

Table 3. Kik-Net stations: peak and cyclic parameters (as provided records)

Station Code	Dir	Level	Epicentral Distance	R_{jb} Distance[4]	PGA	PGAr	PGAk	I_A	S_d
			km	km	*g*	*cm/s²*	*cm/s²*	*cm/s*	*s*
FKSH10	NS	surface	265	97	1.095	1062.4	1062.4	3311.6	48.7
FKSH19	NS	surface	201	52	0.610	605.8	605.8	1622.2	92.9
MYGH10	NS	surface	176	51	0.860	870.8	816.5	3061.8	134.2
TCGH16	NS	surface	298	83	0.805	798.6	774.4	2160.2	69.3
FKSH10	EW	surface	265	97	0.780	768.1	768.1	2022.9	52.3
FKSH19	EW	surface	201	52	0.884	856.6	856.6	2039.6	92.2
MYGH10	EW	surface	176	51	0.844	852.7	804.0	3710.2	115.1
TCGH16	EW	surface	298	83	1.220	1196.7	1196.7	3467.4	37.8
FKSH10	UD	surface	265	97	1.021	1015.8	1015.8	1443.9	59.0
FKSH19	UD	surface	201	52	0.713	729.2	729.2	878.4	237.6
MYGH10	UD	surface	176	51	0.617	622.2	622.2	845.7	164.4
TCGH16	UD	surface	298	83	0.804	807.7	807.7	904.9	153.8
FKSH10	NS	underground	265	97	0.190	179.7	193.5	106.4	172.1
FKSH19	NS	underground	201	52	0.129	130.5	140.6	140.0	254.2
MYGH10	NS	underground	176	51	0.242	218.8	218.8	336.9	237.6
TCGH16	NS	underground	298	83	0.167	176.9	186.3	314.2	259.7
FKSH10	EW	underground	265	97	0.199	135.2	114.8	3167.3	269.5
FKSH19	EW	underground	201	52	0.345	349.8	327.7	117.2	240.5
MYGH10	EW	underground	176	51	0.159	150.2	111.4	1120.5	265.4
TCGH16	EW	underground	298	83	0.221	172.8	260.2	1018.4	266.6
FKSH10	UD	underground	265	97	0.121	86.0	85.8	575.9	267.7
FKSH19	UD	underground	201	52	0.125	126.1	157.2	601.3	268.4
MYGH10	UD	underground	176	51	0.140	107.8	106.1	571.3	263.9
TCGH16	UD	underground	298	83	0.182	137.0	247.4	2325.9	269.4

Table 4. K-Net stations: peak and cyclic parameters (as provided records)

Station Code	Dir	Level	Epicentral Distance	R_{jb} Distance	PGA	PGAr	PGAk	I_A	S_d
			km	km	*g*	*cm/s²*	*cm/s²*	*cm/s*	*s*
MYG004	NS	surface	169	63	2.731	2699.9	2699.9	13350.6	83.0
IBR003	NS	surface	254	33	1.630	1597.6	1599.8	4727.5	24.8
MYG012	NS	surface	169	51	0.830	758.4	869.8	2781.6	243.2
MYG013	NS	surface	175	57	1.549	1517.2	1517.2	1818.5	89.8
MYG004	EW	surface	169	63	1.310	1268.5	1302.3	3988.1	94.1
IBR003	EW	surface	254	33	1.210	1185.9	1187.7	3259.1	35.5
MYG012	EW	surface	169	51	1.985	1969.2	1969.2	2504.9	128.0
MYG013	EW	surface	175	57	1.006	982.3	982.3	1255.5	106.9

[4] The Joyner and Boore distance has been computed considered the following coordinates for the projection of the fault {142.2, 39.9; 144.3, 39.8; 143.3, 36; 141, 36.5} in terms of longitude and latitude for each vertex.

MYG004	UD	surface	169	63	1.923	1879.9	1879.9	2152.2	66.1
IBR003	UD	surface	254	33	1.181	1165.7	1165.7	1334.9	32.7
MYG012	UD	surface	169	51	0.556	500.8	590.1	1694.1	247.3
MYG013	UD	surface	175	57	0.305	290.2	276.3	684.5	225.7

Table 5. Kik-Net stations: peak and cyclic parameters (corrected records)

Station Code	**Dir**	**Level**	**Epicentral Distance**	**R_{jb} Distance**	**PGA**	**PGAr**	**PGV**	**IA**	**ID**	**Sd**
			km	**km**	***g***	***cm/s²***	***cm/s***	***cm/s***		***s***
FKSH10	NS	surface	265	97	1.083	1062.4	34.44	3248.9	55.3	44.1
FKSH19	NS	surface	201	52	0.618	605.8	22.79	1586.8	77.0	90.7
MYGH10	NS	surface	176	51	0.888	870.8	67.22	2704.4	27.0	105.5
TCGH16	NS	surface	298	83	0.814	798.6	68.22	2044.2	22.5	47.1
FKSH10	EW	surface	265	97	0.783	768.1	27.50	2019.0	60.7	52.1
FKSH19	EW	surface	201	52	0.873	856.6	64.38	1979.6	21.9	89.2
MYGH10	EW	surface	176	51	0.869	852.7	44.51	3424.1	57.8	104.3
TCGH16	EW	surface	298	83	1.220	1196.7	82.06	3468.3	21.7	37.6
FKSH10	UD	surface	265	97	1.035	1015.8	25.09	1349.2	32.9	37.4
FKSH19	UD	surface	201	52	0.743	729.2	21.05	445.3	19.1	82.2
MYGH10	UD	surface	176	51	0.634	622.2	16.51	686.7	45.9	94.1
TCGH16	UD	surface	298	83	0.823	807.7	28.89	722.8	18.6	15.9
FKSH10	NS	underground	265	97	0.183	179.7	18.28	83.5	15.1	47.7
FKSH19	NS	underground	201	52	0.133	130.5	7.42	46.3	33.2	82.9
MYGH10	NS	underground	176	51	0.223	218.8	26.19	175.1	18.8	100.9
TCGH16	NS	underground	298	83	0.180	176.9	27.18	80.3	10.7	71.7
FKSH10	EW	underground	265	97	0.138	135.2	9.38	54.3	27.2	54.2
FKSH19	EW	underground	201	52	0.357	349.8	16.85	57.3	6.1	80.2
MYGH10	EW	underground	176	51	0.153	150.2	16.64	147.3	34.2	107.8
TCGH16	EW	underground	298	83	0.176	172.8	18.94	100.7	18.2	56.4
FKSH10	UD	underground	265	97	0.088	86.0	11.64	40.8	25.3	65.5
FKSH19	UD	underground	201	52	0.129	126.1	11.14	29.9	14.0	87.5
MYGH10	UD	underground	176	51	0.110	107.8	10.48	92.8	50.1	107.5
TCGH16	UD	underground	298	83	0.140	137.0	13.93	46.6	16.5	85.1

Table 6. K-Net stations: peak and cyclic parameters (corrected records)

Station Code	**Dir**	**Level**	**Epicentral Distance**	**R_{jb} Distance**	**PGA**	**PGAr**	**PGV**	**IA**	**ID**	**Sd**
			km	**km**	***g***	***cm/s²***	***cm/s***	***cm/s***		***s***
MYG004	NS	surface	169	63	2.908	2699.9	109.75	13113	26.2	80.9
IBR003	NS	surface	254	33	1.687	1597.6	65.03	4703.4	27.3	24.8
MYG012	NS	surface	169	51	0.681	758.4	33.38	1245.7	34.9	107.6
MYG013	NS	surface	175	57	1.463	1517.2	85.76	1803.4	9.1	89.7
MYG004	EW	surface	169	63	1.218	1268.5	47.97	3844.4	41.9	84.7
IBR003	EW	surface	254	33	1.226	1185.9	42.91	3239	39.2	35.5
MYG012	EW	surface	169	51	1.906	1969.2	51.44	2241.3	14.5	103.3
MYG013	EW	surface	175	57	0.943	982.3	46.64	1234.1	17.9	106.6
MYG004	UD	surface	169	63	1.948	1879.9	38.90	2106.1	17.7	64.0
IBR003	UD	surface	254	33	1.113	1165.7	26.61	1272.1	27.3	30.0
MYG012	UD	surface	169	51	0.491	500.8	21.01	723.24	44.6	110.3
MYG013	UD	surface	175	57	0.299	290.2	20.41	430.87	45.0	103.5

Table 7. BRI stations: peak and cyclic parameters (as provided records)

Station Code	**Dir**	**Level**	**Epicentral Distance**	**R_{jb} Distance**	**PGA**	**PGAr**	**PGV**	**IA**	**ID**	**Sd**
			km	**km**	***g***	***cm/s²***	***cm/s***	***cm/s***		***s***
SND	74	BF2	175	62	0.166	163.3	44.2	205.4	17.8	119.7
SND	164	BF2	175	62	0.264	259.0	34.2	297.6	21.0	115.2
SND	UP	BF2	175	62	0.150	147.0	20.1	149.9	31.7	114.0
HCN2	164	GL	292	91	0.291	285.6	19.8	544.5	60.1	92.9
HCN2	254	GL	292	91	0.214	210.3	17.0	308.5	53.9	100.3
HCN2	UP	GL	292	91	0.062	60.9	6.6	36.3	56.0	106.5

5. Elastic Spectra

The elastic acceleration spectra have been evaluated at 25 periods, the smallest is 0.03 seconds, and the highest is 4.0 seconds. The elastic spectra are investigated employing Kik-Net and K-Net corrected records and uncorrected BRI records. Figure 3 and Figure 4 shows the spectra for Kik-Net stations surface and underground records respectively, both horizontal and vertical spectra are considered. Figure 5 shows the spectra for K-Net stations and Figure 6 for BRI stations.

It has to be noted that records from K-Net network are characterized by specific high spectral value that cannot be recognized in Figure 5 because of the 5g scale adopted for all the acceleration spectra allowing a better comparison between all the records selected. MYG004 registration have a peak in the NS component, among the 25 periods investigated here, at 0.25 seconds equal to 11.98 g while the peak spectral value in EW component is significantly lower, 4.31 g at 0.2 seconds. MYG004 vertical component is characterized by a single spectral value equal to 6.15 g at 0.1 seconds that as well cannot be recognized because of the scale adopted in Figure 5.

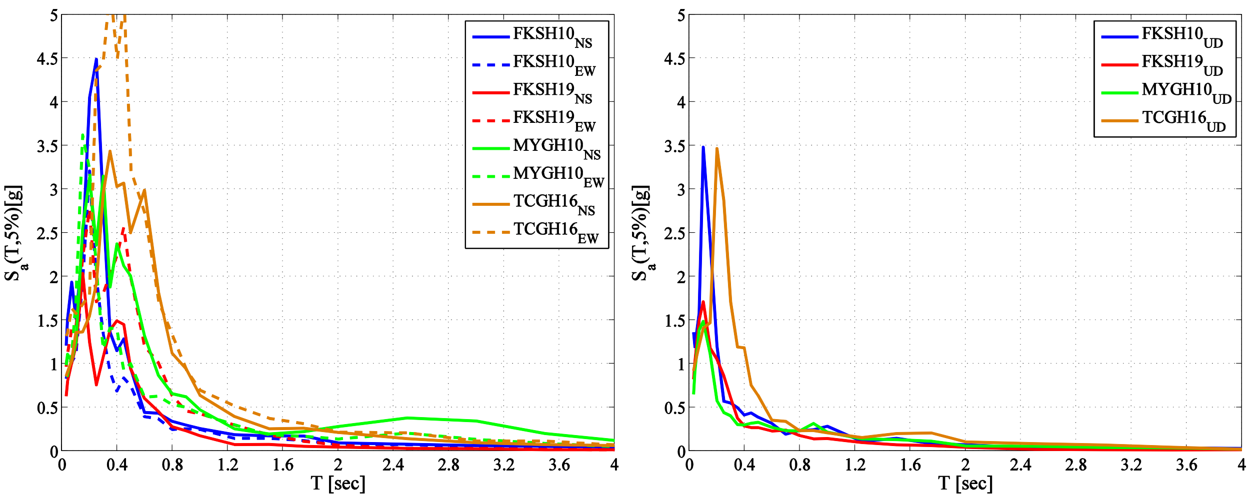

Figure 3. Elastic spectra of horizontal (left) and vertical (right) components Kik-net, (surface)

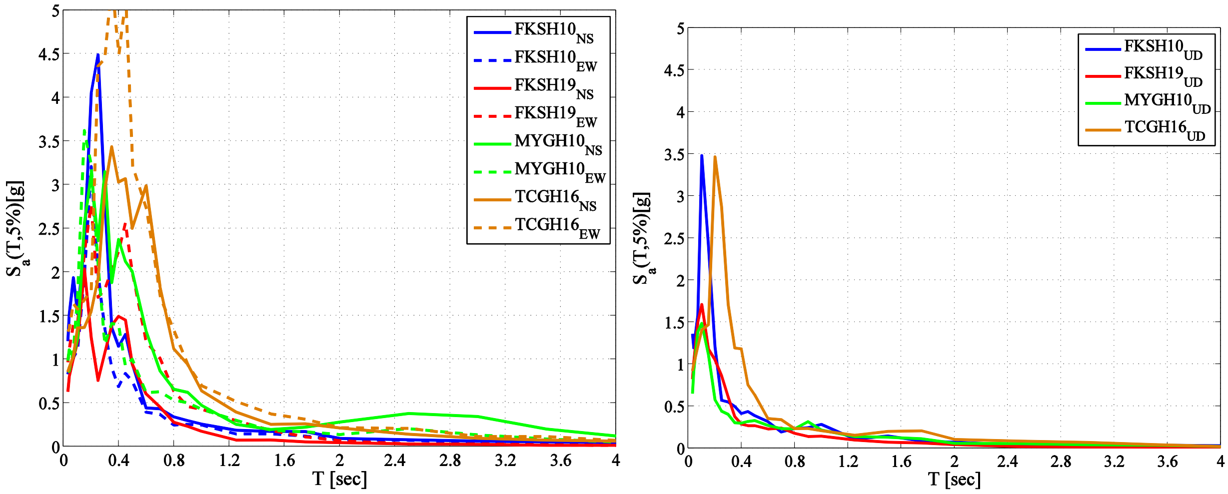

Figure 4. Elastic spectra of horizontal (left) and vertical (right) components, Kik-net (underground)

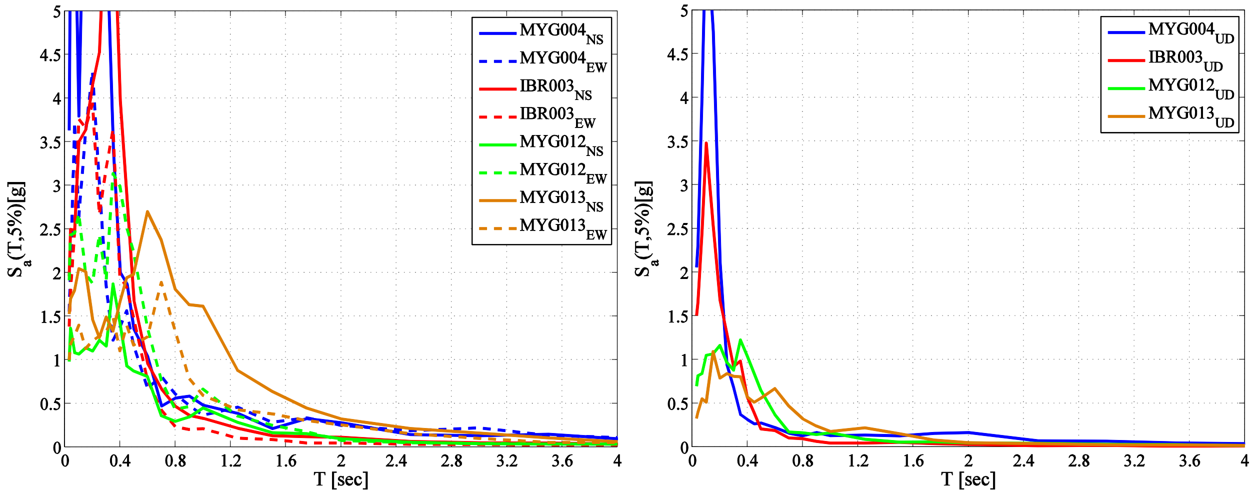

Figure 5. Elastic spectra of horizontal (left) and vertical (right) components, K-net

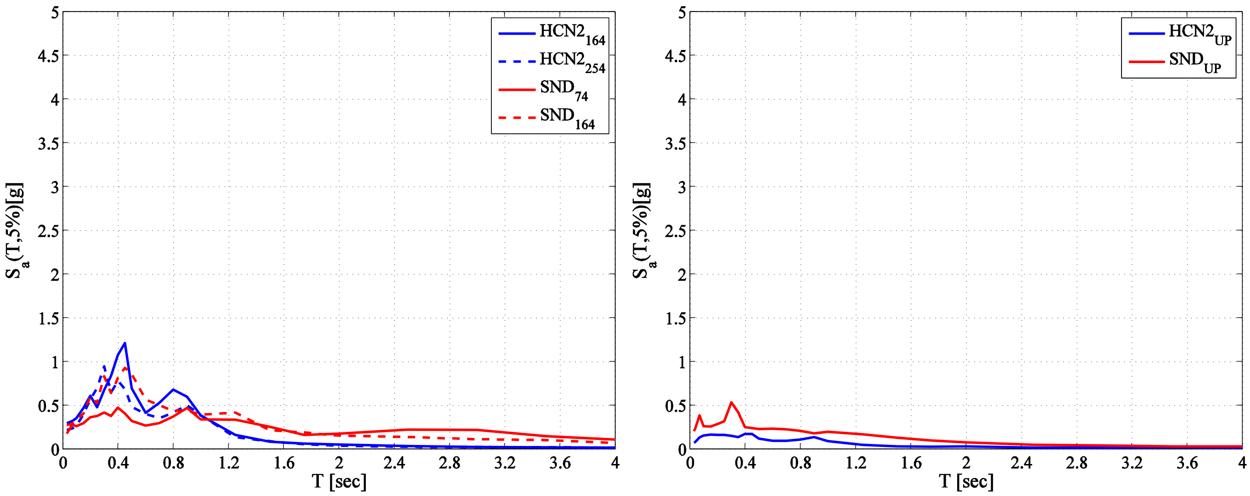

Figure 6. Elastic spectra of horizontal (left) and vertical (right) components, BRI.

6. Fault-Normal and fault-parallel components

A report of National Research Institute for Earth Science and Disaster Prevention (NIED, 2011) provided some preliminary information about the rupture fault model; such data, in particular the suggested strike angle, equal to 195°, allowed rotating to fault-normal (FN) and fault-parallel (FP) the corrected components of the selected records, from K-Net and Kik-NET (surface records). This means to get strike-normal and strike-parallel components, respectively. The same peak and integral parameters of the previous section have been evaluated for the rotated components. Table 7 and 8 show the results for Kik-Net and K-Net respectively.

Table 7. Kik-Net stations: peak and cyclic parameters for the rotated components, (surface)

Station Code	Dir	Level	Epicentral Distance	R_{jb} Distance	PGA	PGV	IA	ID	Sd
			km	km	*g*	*cm/s*	*cm/s*		*s*
FKSH10	FN	surface	265	97	0.737	25.79	1898.0	63.6	53.4
FKSH19	FN	surface	201	52	0.882	66.55	2132.7	23.1	89.0
MYGH10	FN	surface	176	51	0.847	45.66	3269.0	53.8	104.3
TCGH16	FN	surface	298	83	1.268	85.84	3705.8	21.7	37.9
FKSH10	FP	surface	265	97	1.096	35.13	3369.9	55.7	44.3
FKSH19	FP	surface	201	52	0.585	20.65	1433.8	75.6	91.2
MYGH10	FP	surface	176	51	0.880	61.42	2859.5	33.7	104.4
TCGH16	FP	surface	298	83	0.774	63.04	1806.7	23.6	51.2

Table 8. K-Net stations: peak and cyclic parameters for the rotated components

Station Code	Dir	Level	Epicentral Distance	R_{jb} Distance	PGA	PGV	IA	ID	Sd
			km	km	*g*	*cm/s*	*cm/s*		*s*
MYG004	FN	surface	169	63	1.399	56.10	4617.7	37.5	82.3
IBR003	FN	surface	254	33	1.555	48.49	3623.1	30.6	34.6
MYG012	FN	surface	169	51	1.825	52.22	2077.3	13.9	101.2
MYG013	FN	surface	175	57	0.722	54.41	1216.8	19.7	102.7
MYG004	FP	surface	169	63	2.896	106.10	12339.7	25.6	81.0
IBR003	FP	surface	254	33	1.647	66.50	4319.3	25.1	24.7
MYG012	FP	surface	169	51	0.750	30.41	1409.7	39.4	110.3
MYG013	FP	surface	175	57	1.658	78.83	1820.7	8.9	96.5

Rupture directivity effects may interest near-source records resulting in peculiar velocity signals characterized by a large pulse in the beginning of the record. Usually such effects are studied in FN and FP directions: in fact FN is the direction in which they are supposed to be higher (Somerville, 2005). Due to the rupture dimensions, all the considered stations are within the near-source area but analyzing rotated components with a quantitative algorithm, proposed by Baker (Baker, 2007), no record has been classified as *pulse-like*. It is worth to note that, referring to the direction of surface displacement, all the stations are seems to be in conditions not favourable to observe forward directivity.

7. Comments

MYG stations from both K-net and Kik-net and Sendai government building (SND) are close to each other (see Figure 2) and they are the closest to the epicentre among those considered. This area was also stroked by the tsunami event following the earthquake and produced catastrophic effects. MYG stations are located within 200 km from the epicentre. If these data will be confirmed, the most peculiar result is the PGA of the NS component of MYG004 station (169 km) belonging to K-Net network; this PGA is equal to 2.91 g, while the PGA of the same record in the EW direction is approximately half this value (1.45 g).

The other MYG signals are equally close to the epicentre. MYGH10 record (surface), which belongs to Kik-Net network, (176 km) do not show any evident discrepancy between the PGA of the NS and EW components (0.89 g versus 0.87 g).

MYG012 record, which belongs to K-Net, as well as MYG004 record, shows a similar effect to the one observed in MYG004 in EW component even if the value of the maximum PGA is significantly lower. In fact, the PGA of the EW component of MYG012 is equal to 1.90 g, more than double of the 0.68 g found in the NS component. Aimed at a better comparison of these results, in Figure 7 and Figure 8 the acceleration and velocity time-histories of MYG004 MYG012 and MYGH10 (surface) are shown together considering the corrected waveforms. The comparison of acceleration and velocities time-histories does not suggest any evident atypical trend in the signals, these plots help emphasizing that the NS component of MYG004 record is significantly higher with respect to all the other components of the three records registered close to each other. Further investigations are needed for these records.

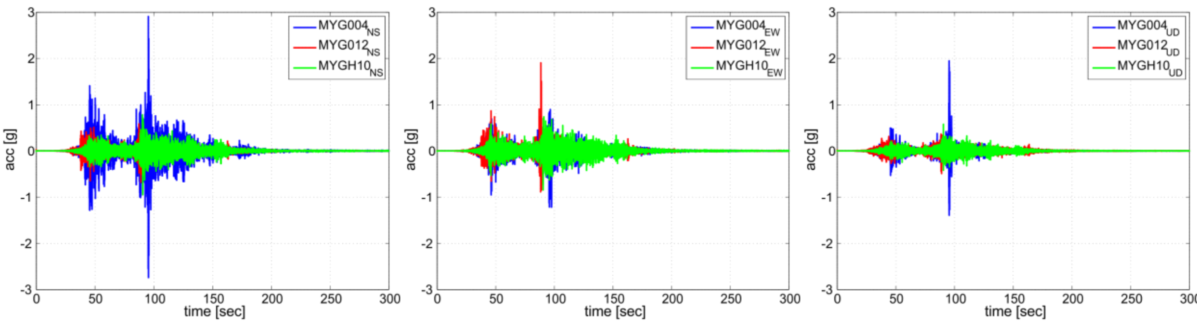

Figure 7. Comparison between acceleration time-histories of MYG004, MYG012 and MYGH10 records for NS, EW and UD components (corrected records).

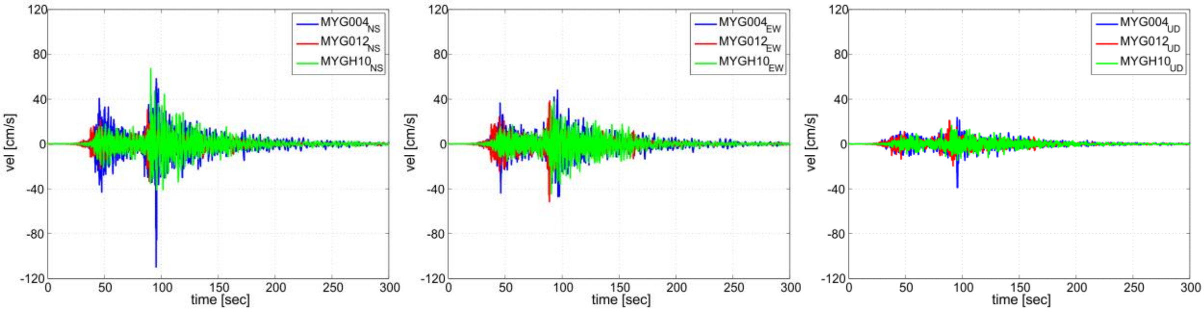

Figure 8. Comparison between velocity time-histories of MYG004, MYG012 and MYGH10 records for NS, EW and UD components (corrected records).

In this comparison SND signal from BRI network was not included even if it was registered very close to the other three stations (epicentral distance equal to 175 km). SND showed a very low value of PGA respect to the others in both components (0.26 g and 0.16 g) but it was registered in a building and no information are available regarding the structure and the placement of the sensors that certainly had a strong effect on the registration.

Another peculiar effect that can be observed in the results showed in the previous sections is the significant difference between elastic spectra of surface and underground records (see Figure 3 and Figure 4). Underground records have been registered between 100 to 200 meters under the surface registration (see Table 1) and they come from the same network, Kik-net, so they are characterized by the employment of the same kind of instruments. The amplification appears always very significant. Unfortunately, Kik-Net network does not provide the velocity profile and soil columns of the stations that could have helped in a straightforward interpretation of the amplification effect due to geotechnical characteristics of the soil; on the other hand the underground registrations are obtained at significant depth, larger than the average column depth employed for geotechnical characterization of the station (approximately equal to 30 meters).

Elastic spectra in Figure 3 and Figure 4 show that the most of the amplifications occur in the last 100-200 meters, and PGA of the underground signal can be considered comparatively low. It is worth to note that underground record peak values and their elastic spectra are comparable with the values registered on buildings (from BRI network). As in the previous case for SND registration compared with the other close registration, it is not easy to explain this deamplification effects registered on the two buildings considered, since no information are available regarding the structural systems of the buildings.

In the case of the four K-Net stations the soil columns and the velocity profiles are known (Table 2). IBR003 station is characterized by the lowest velocity profile between the four stations compared, so an higher spectral amplification is expected and confirmed by the results shown in Figure 5 (also considering that this station is characterized by an epicentral distance of 254 km).

MYG004 station, that registered the highest peak of acceleration (2.73 g), is characterized by high values of velocity in the profile and rock, very stiff, soil is found at less than 5 meters from the surface. The clay layer, less than 5 meters thick, can suggest the presence of an S1 or S2 soil according to the definition of Eurocode 8 [CEN, 2003], but this needs further investigations.

The information provided herein are very preliminary, therefore the above comments represents simply guidance for further investigations and are not meant to be conclusions regarding this earthquake which requires much deeper analyses.

References

Baker J.W. Quantitative classification of near-fault ground motions using wavelet analysis. Bulletin of the Seismological Society of America 2007; 97(5), 1486–1501

BRI strong motion observation, 2011, http://smo.kenken.go.jp/weblinks

CEN, 2003, Eurocode 8: design of structures for earthquake resistance – Part 1: general rules, seismic actions and rules for buildings, European Standard EN 1998-1:2003. Comité Européen de Normalisation, Brussels.

Cosenza E., Manfredi G., Ramasco R, 1993: The Use of Damage Functionals in Earthquake Engineering: A Comparison between Different Methods. Earthquake Engineering and Structural Dynamics, 22(10), 855-868.

Kik-net, 2011, Digital Strong-Motion Seismograph Network http://www.kik.bosai.go.jp/

K-net, 2011, Kyoshin Network http://www.k-net.bosai.go.jp/

NIED, 2011, 2011 Off the Pacific Coast of Tohoku Earthquake, Strong Ground Motion, available at http://www.reluis.it/images/stories/Rapporto_Kik-Net.pdf

Somerville PG. Engineering characterization of near-fault ground motions. Proceedings of 2005 NZSEE Conference, Wairakei, NZ, 2005.

USGS website, 2011, http://www.usgs.gov/

Zollo A., 2011, “I terremoti giganti”, (in Italian), available at http://www.scienzainrete.it/contenuto/articolo/i-terremoti-giganti